Thermogravimetric Analysis of the Effects of Transition Metals on the Co-pyrolysis of Rice Straw and Polyethylene

Guofu Liu,[a,#] Zhanghong Wang,[a,b,#] Dekui Shen,[a,*] Chunfei Wu,[c,*] and Sai Gu [d]

Different transition metals (Ni, Co, Fe, and Mn) at different amounts (0 mmol/g to 1 mmol/g) were introduced into the co-pyrolysis of rice straw and polyethylene. The thermal behavior and the kinetics of rice straw, polyethylene, transition metal-treated rice straw, rice straw/polyethylene, and transition metal-treated rice straw/polyethylene were comparatively investigated *via* thermogravimetric analysis. The Ni, Co, Fe, and Mn promoted the decomposition of rice straw and polyethylene in mixtures compared with non-transition metal-treated mixtures in terms of the initial decomposition temperature. The presence of these transition metals catalyzed the synergistic interaction between the rice straw and the polyethylene in mixtures, which resulted in a reduction of residue yield from 14.9 wt% for rice straw/polyethylene to 12.6 wt% to 14.5 wt% for transition metal-treated mixtures. Moreover, the difference in weight loss suggested that the negative influence of the softened polyethylene on the rice straw in mixtures could be greatly reduced after the involvement of transition metals. Kinetic analysis revealed that the pyrolysis of rice straw, polyethylene, and transition metal-treated rice straw were well fit by a single first order reaction; two consecutive first order reactions were needed to describe the co-pyrolysis of rice straw/polyethylene with or without transition metals.

Key words: Co-pyrolysis; Rice straw; Polyethylene; Transition metal; Thermogravimetric analysis

Contact information: a: Key Laboratory of Energy Thermal Conversion and Control of Ministry of Education, Southeast University, Nanjing 210096, PR China; b: School of Engineering and Computer Science, University of Hull, Hull HU6 7RX, United Kingdom; c: School of Chemistry and Chemical Engineering, Queen's University Belfast, Belfast BT7 1NN, United Kingdom; d: Faculty of Engineering and Physical Sciences, University of Surrey, Guilford, GU2 7XH, United Kingdom;
** Corresponding authors: 101011398@seu.edu.cn; c.wu@qub.ac.uk;*
[#] These two authors contribute equally to the manuscript

INTRODUCTION

Agricultural waste is an inevitable class of biomass, which accompanies the harvest of agricultural crops and needs to be disposed of immediately and efficiently in order to ensure normal production during the next season. China is a large agricultural country, responsible for a large amount of agricultural waste output every year. Qiu *et al.* (2014) stated that the theoretical amount of agricultural waste output in China in 2010 was as high as 729 million tons, and the collectable quantity was more than 600 million tons. The direct incineration of these agricultural waste products, one of the most utilized disposal methods in the past few decades, was found to be seriously responsible for air pollution (*e.g.*, sulfur dioxide, nitrogen dioxide, and allergens) and soil degradation (*e.g.*, water loss, microbial death, and soil agglomeration). Consequently, it is important to explore and develop more effective and environmentally friendly ways to dispose of

these large amounts of resources. In recent years, pyrolysis has been gradually developed in terms of converting agricultural wastes into bio-fuels (bio-oil). Such conversion not only serves as an effective way to dispose of agricultural waste, but it also produces renewable energy to meet the continuously increasing energy demand of daily life (Sipra *et al.* 2018). However, it is noticeable that bio-oil obtained from the pyrolysis of agricultural wastes possesses some critical drawbacks, which greatly hinder further development; such as low calorific value, a low pH value, high oxygen levels, and high viscosity (Zhang *et al.* 2016). Therefore, the agricultural waste-derived bio-oil generally must be modified to improve its quality prior to usage as a valuable fuel (Zhang *et al.* 2013).

More recently, attention has been given to the production of high-quality bio-oil *via* the introduction of a catalyst (catalytic pyrolysis) and the co-feeding of hydrogen-rich feedstock (co-pyrolysis) during the pyrolysis process in a single-step process (Zhang *et al.* 2016; Xiang *et al.* 2018). In the case of catalytic pyrolysis, a catalyst being employed could provide active sites to promote the deep decomposition of feedstock and intensify the interaction between the intermediates *via* the formation of hydrocarbon radical pools, which results in an improvement of the reaction efficiency and the quality of the bio-oil (Fermoso *et al.* 2016). Besides active sites, the distinctive pore structure of the catalyst, especially for zeolites-assorted catalysts, was also found to play an important role in the selective production of high-quality bio-oil (Hernando *et al.* 2016). However, due to the low effective hydrogen to carbon ratio ($H/C_{effective}$) of the biomass, the yields of the desired compounds in bio-oil obtained from catalytic pyrolysis are still relatively low. Meanwhile, the high rate formation of coke during this process also gives rise to a rapid deactivation of the catalyst.

A co-pyrolysis technique with the addition of H-rich feedstock, such as ethanol or plastics, during the biomass pyrolysis process has also been found to be effective for the improvement of the quality of biomass-derived bio-oil (Dorado *et al.* 2015). The involvement of co-feeding components primarily played a role in providing a large amount of H or hydrocarbon free radicals to promote the cleavage of O-containing compounds and directly interact with the biomass-derived intermediates (Zhang *et al.* 2016). However, the low reaction efficiency of the interaction between the biomass and the H-rich feedstock, and the interactions between the intermediates highly limit the yield of valuable components and the conversion efficiency of the feedstock.

In terms of their individual advantages of improving the quality of the biomass-derived bio-oil, the combination of catalytic pyrolysis with co-pyrolysis, namely catalytic co-pyrolysis, has subsequently been developed (Wang *et al.* 2018). In a catalytic co-pyrolysis process, it is expected that the H-rich additives could provide sufficient H-containing compounds, while the interaction between the biomass derived intermediates and the H-rich additives could be greatly promoted by the catalyst (Li *et al.* 2014). According to the report of Lee *et al.* (2016), a strong synergistic effect was observed during the pyrolysis of torrefied cellulose with polypropylene over HZSM-5. The maximum benzene, toluene, ethylbenzene, and xylene (BTEX) yield obtained from the catalytic co-pyrolysis of torrefied cellulose/polypropylene was 33.4 wt%, which was higher than the catalytic pyrolysis of torrefied cellulose (23.7 wt%) (Lee *et al.* 2016). Compared to the co-pyrolysis of polypropylene and *Laminaria japonica* in the absence of catalyst, the process with the treatment of Pt/mesoporous MFI molecular sieve showed a dramatic decrease in the oxygenates content against the substantial increase in the aromatics content (Kim *et al.* 2017). Therefore, catalytic co-pyrolysis is a feasible,

efficient, and promising technique for the production of high-quality biomass-based bio-oil.

Transition metals can be efficient and cost-effective catalysts. They have been applied in various fields such as the catalytic pyrolysis of biomass for the preparation of carbon-based materials, bio-oils, syngas, or chemicals (Collard *et al.* 2012; Thompson *et al.* 2015). It is unclear whether transition metals act as efficient catalysts between biomass and H-rich feedstock during co-pyrolysis, which could lead to changes in products distribution, bio-oil quality and yield, and high value-added compounds selectivity. To date, there has been limited research in this area. To illuminate the thermal behavior and the kinetics of the catalytic co-pyrolysis of biomass and H-rich feedstock with the addition of transition metals is intuitive and necessary. Accordingly, the purpose of the present study was to investigate the influence of transition metals treatment on the co-pyrolysis process *via* TGA. Particularly, rice straw (RS) and polyethylene (PE) were employed as the typical representatives of agricultural wastes and H-rich feedstock, respectively. The thermal behavior and the kinetics of the RS and PE co-pyrolysis influenced by the type of transition metal (Ni, Co, Fe, and Mn) and the concentration of the transition metal (Ni) were exhaustively investigated *via* TGA at room temperature to 850 °C under a N_2 atmosphere.

EXPERIMENTAL

Materials

Rice straw was collected from a farm in Nanjing, China, was cut into chops, washed with water, then sun-dried to remove most of the natural moisture. The sun-dried RS was oven-dried at 105 °C, ground, and sieved. The RS powder particles with a diameter smaller than 0.45 μm were collected. The PE powder and the transition metal nitrates (AR) were purchased from the Sigma-Aldrich Corporation (St. Louis, MO, USA).

Experimental Procedure

Characterization of RS and PE

The three main polymer components of RS**,** *i.e.* lignin, cellulose, and hemicellulose, were determined according to the methodology by Wang *et al.* (2016) after a Soxhlet extraction pre-treatment to remove the extractives. An approximate analysis was tested according to ASTM 1762-84 using an oven and muffle furnace. The Ultimate analysis was performed using an Elemental Analyzer (Thermo Finnigan, EA 112, San Jose, CA, USA). The exact mineral content in the RS, which mainly consisted of alkali and alkaline earth metals (potassium (K), sodium (Na), calcium (Ca), and magnesium (Mg)) and transition metals (Ni, Co, Fe, and Mn), was determined using an inductively coupled plasma-atomic emission spectrometry (ICP-AES) (Perkin-Elmer, Optima Plasma 3200 RL, Waltham, MA, USA) after the RS digestion, according to US EPA method 6010.

Sample preparation

First, the transition metal-treated RS was prepared. It was mixed with PE, and the desired metal-treated RS/PE mixture was collected (Wang *et al.* 2018). In detail, 1 g of

RS powder was added into a 20 mL transition metal-containing solution with a transition metal concentration of 0.1 mol/L. The suspension was vigorously stirred at 60 °C to evaporate most of the water and then transferred into an oven to dry at 105 °C. The dried powder was collected and mixed with 1 g of PE powder in an agate mortar *via* manual grinding for 20 min. The ground powder was a targeted mixture of RS and PE in a ratio of 1:1 with a transition metal concentration of 1 mmol/g. The prepared transition metal-treated RS/PE mixtures were labeled as RS/PE-Ni-1, RS/PE-Co-1, RS/PE-Fe-1, and RS/PE-Mn-1, respective to their used transition metals. Rice straw/polyethylene mixtures with different transition metal concentrations (Ni in a concentration from 0 mmol/g to 1 mmol/g) were also prepared in a similar process, which were denoted to as RS/PE-Ni-0, RS/PE-Ni-0.25, RS/PE-Ni-0.5, RS/PE-Ni-75, and RS/PE-Ni-1. For comparison, a RS/PE mixture without the catalyst and RS mixtures with 1 mmol/L of the transition catalyst (*i.e.*, RS-Ni-1, RS-Co-1, RS-Fe-1, and RS-Mn-1) were prepared as well.

Thermogravimetric analysis

The pyrolysis data of the RS and the PE, as well as their mixtures with or without transition metals, were derived from the pyrolysis experiments conducted in a thermogravimetric analyzer (Mettler Toledo, 188 TGA/SDTA 851, Greifensee, Switzerland). Approximately 10 mg of the sample was loaded into an aluminum oxide crucible and pyrolyzed under a 0.1 m^3/min N_2 flow at a heating rate of 10 °C/min. The weight change of the sample with the function of temperature (ambient temperature (°C) to 850 °C) and time consumed were collected. Consequently, the weight loss (TG) and weight loss rate (DTG) with the increase in temperature were calculated according to Eq. 1 and Eq. 2, respectively,

$$\eta = 100\% \times \frac{W_0 - W_{temperature}}{W_0} \quad (1)$$

$$\varphi = \frac{d\eta}{dt} \quad (2)$$

where W_0 (mg) is the initial mass of sample and $W_{\text{temperature}}$ (mg) is the mass at temperature T, and t (min) is the time corresponding to the temperature. Three parallel runs were carried out for all the experiments to ensure low relative errors (below 5%).

Kinetic Study

Kinetic parameters including the activation energy and the pre-exponential factor were calculated according to the TGA data, which can be utilized to qualitatively reveal the thermal conversion characteristics of the feedstock. It was reported by Xiong *et al.* (2015) and Wang *et al.* (2018) that the pyrolysis of the biomass and the plastics primarily followed a first order model reaction, which can be expressed as Eq. 3,

$$\frac{dx}{dt} = A\exp[(\frac{-E}{RT})(1-x)] \quad (3)$$

where E is the activation energy (kJ/mol), A is the pre-exponential factor (1/min), T is the temperature (K), and R is the universal gas constant (J/mol K). The conversion of feedstock, x, was calculated using Eq. 4,

$$x = \frac{W_0 - W_{time}}{W_0 - W_{final}} \quad (4)$$

where W_{time} is the mass of the sample at time t and W_{final} is the mass of the sample at the end of pyrolysis. When a constant heating rate H (H=dT/dt) is applied, Eq. 3 can be integrated as Eq. 5,

$$\ln[\frac{-\ln(1-x)}{T^2}] = \ln[\frac{AR}{HE}(1-\frac{2RT}{E})] - \frac{E}{RT} \quad (5)$$

where due to RT/E being much less than 1 in general, the expression ln[AR / HE(1-2RT / E)] can be regarded as a constant. As a result, E and A can be calculated from the slope and the intercept of the plots of ln[-ln(1-x)/T^2] versus 1/T, respectively.

Interaction Investigation

The interaction between the individual fractions in the mixture can be revealed by investigating the difference in weight loss (ΔW) between the experimental values and the theoretical ones, according to Wang *et al.* (2018), as shown in equation Eq. 6,

$$\Delta W = W_{mixture} - (x_1 W_1 + x_2 W_2) \quad (6)$$

where $W_{mixture}$ is the weight loss of RS/PE mixture with or without transition metals, which was obtained from the TGA experiment, and $x_1W_1 + x_2W_2$ represents the theoretical weight loss of the corresponding mixture derived from calculation. Particularly, x_1 and x_2 are the weight fraction of RS and PE in the mixtures, respectively, and W_1 and W_2 are the weight loss of the RS with or without the transition metal treatment and PE, respectively. In principle, ΔW would close to zero if no interaction between the individual fractions occurred.

RESULTS AND DISCUSSION

Physicochemical Properties of the Raw Materials

The physicochemical properties investigated *via* means of composition analysis, proximate analysis, ultimate analysis, minerals, and gross calorific value are presented in Table 1. It can be seen that RS primarily consisted of lignins, cellulose, and hemicellulose, which was comparable to other studies (Table 1) (Zhang *et al.* 2017; Castro *et al.* 2017). The lignin content in RS is considered important to the fixed carbon content of RS (6.75 wt%), while a high volatile matter content (70.85 wt%) is generally related to its cellulose and hemicellulose content. In comparison, PE is comprised of a negligible amount of fixed carbon and ash compared to its high volatile matter level (greater than 98%). According to ultimate analysis, the RS contained a high level of O and a relatively low level of N and S in addition to the C and H content, while the PE was only composed of C and H. It was reported that the high O content in fuel could negatively affect its heat value, which can be confirmed by the gross calorific value of RS and PE (Hernando *et al.* 2016). Furthermore, the $H/C_{effective}$ ratio of PE was 2.18, which was much higher than that of the RS (0); this indicated that the combination of PE with RS would greatly improve the $H/C_{effective}$ of the RS-based feedstock. Mineral analysis revealed that the RS contained a large amount of alkali and alkaline earth metals,

especially K (13.55 mg/g) against negligible transition metals. Yang *et al.* (2006) found that the presence of K in the biomass could act as a catalyst to facilitate the thermochemical decomposition of the biomass. Accordingly, the pyrolysis performance of the RS and the mixture together with the PE may be influenced by the intrinsic K content of the RS to a certain degree.

Table 1. Physicochemical Properties of RS and PE

Composition Analysis								
	Lignin (wt%)		Cellulose (wt%)		Hemicellulose (wt%)			
RS (present study)	15.4		35.9		29.2			
RS in Zhang *et al.* (2017)	16.4		36.1		24.7			
RS in Castro *et al.* (2017)	17.5		35.3		23.8			
Proximate Analysis								
	Fixed Carbon (wt.%)		Volatile Matter (wt%)		Ash (wt%)		Moisture (wt%)	
RS	6.75		70.85		14.6		5.01	
PE	0.32		98.12		0.18		0.52	
Ultimate Analysis								
	C (%)	H (%)	O (%)[a]	N (%)	S (%)	$H/C_{effective}$[c]	GCV (MJ/Kg) [d]	
RS	40.21	5.46	52.89	0.92	0.28	0	11.96	
PE	84.64	15.36	[b]	-	-	2.18	50.79	
Minerals								
	K (mg/g)	Na (mg/g)	Ca (mg/g)	Mg (mg/g)	Ni (mg/Kg)	Co (mg/Kg)	Fe (mg/Kg)	Mn (mg/Kg)
RS	13.55	1.03	3.18	1.23	-	`-	0.4	-
a is calculated from the mass difference (O% = 100% − C% − H% − N% − S%)								
b represents below detectable limitation								
c $H/C_{effective}$ was calculated from the equation; $H/C_{effective}$ = (H-2O-3N-2S)/C								
d The gross calorific value (GCV) of RS and PE was calculated according to Dulong's equation *i.e.*, GCV(MJ/Kg) = 0.3383 C + 1.422 (H-O/8) + 0.095 S								

Pyrolysis Characteristics

RS with or without transition metals, PE, and RS/PE mixture

Figure 1 shows the TG and DTG curves of the RS mixtures with or without transition metals, PE, and RS/PE during pyrolysis. It was found that the decomposition process of the RS can be generally divided into three stages. The first stage ranged from room temperature (°C) to 190 °C with a 8.1 wt% weight loss that was attributed to the loss of the adsorbed free water along with the release of some small molecular weight compounds such as gas molecules (CO, CO_2, H_2, and CH_4) and organic acids (*e.g.*, formic acid) (Kai *et al.* 2017). This can be indirectly confirmed by the moisture content obtained from a proximate analysis (5.0 wt%), which was lower than the weight loss at this stage and indicated that the weight loss in this stage contained not only water but also additional compounds. After that, the RS undergoes a rapid weight loss stage, which commences at 190 °C and ends at 361 °C, which accounted for 69.2 wt% of the total weight loss of the RS during the whole pyrolysis process. Uzun and Yaman (2017) stated that the decomposition of hemicellulose, cellulose, and lignins primarily takes place in the temperature ranges of 230 °C to 325 °C, 310 °C to 400 °C, and 160 °C to 900 °C, respectively. The complete decomposition of the hemicellulose and the cellulose as well as the partial decomposition of the lignins are responsible for the rapid weight loss of the

RS at this stage. However, the rapid weight loss stage of the RS was reflected in the DTG curve (as shown in Fig. 1b) as a distinct weight loss peak with a maximum weight loss rate of -5.86 wt%/min at 310 °C. It was likely that the weight loss peak at this temperature originated from the drastic decomposition of cellulose, since the weight loss peak of the hemicellulose in the biomass matrix generally occurred around 270 °C and was observed as a shoulder peak of the cellulose (Garba *et al.* 2018). The concentration of hemicellulose is the lowest compared to lignin and cellulose in RS (Table 1). The decomposition peak of hemicellulose could not be clearly observed, which may have arisen from the presence of minerals (such as K), which resulted in the overlap of the pyrolysis peak. After the rapid weight loss stage, the decomposition of RS underwent a slow weight loss stage from 361 °C to 850 °C with a 13.3 wt% weight loss, which was attributed to the carbonization process of the cellulose and hemicellulose residue and the slow pyrolysis of the lignin.

After the transition metal treatment (RS-Ni-1, RS-Co-1, RS-Fe-1, and RS-Mn-1), the variation trend of the pyrolysis curves were in accordance with that of RS, but the weight loss at the first stage was slightly higher (except for RS-Co-1). A possible explanation is that the involvement of transition metals could enhance the hydrophilicity of the RS. Collard *et al*. (2015) found that a transition metal treatment led to a decrease in the number of hydrogen bonds in the biomass and partly promoted the transformation of the crystalline components into amorphous phase ones, which resulted in more water content being involved in the transition metals-treated RS. The main decomposition stage of the transition metal-treated RS seemed to vary with the type of transition metal. The decomposition of RS-Ni-1, RS-Co-1, RS-Fe-1, and RS-Mn-1 at this stage started at 194 °C, 197 °C, 176 °C, and 199 °C, respectively, and the weight loss peaks occurred at 321 °C, 309 °C, 306 °C, and 309 °C, respectively. This indicated that the interaction the between transition metal and the RS was affected by the type of metal. Wang *et al.* (2018) considered that the introduction of transition metal ions to cellulose acted as Lewis acid sites and played an important role in the dehydration and the depolymerization of the cellulose. Consequently, the initial decomposition temperature of the transition metal-treated cellulose exhibited a negative relationship with the Lewis acidity intensity of the transition metal employed (Mn was greater than Ni, which was greater than Co, which was greater than Fe). This conclusion was not applicable for the present work, due to the RS sample being composed of cellulose, hemicellulose, lignin, ash, and extractives, which was more complex than the biomass used in Wang *et al.* (2018). It is worth noting that among all transition metal-treated RS, RS-Ni-1 possessed a weight loss shoulder peak at 265 °C, which was also assigned to the rapid decomposition of hemicellulose. This observation further demonstrated the different catalytic behavior of the various transition metals. In addition, the residue of the RS (100% weight loss) with a transition metal treatment after the final slow decomposition stage at 850 °C was in the range of 30.9 wt.% to 34.2 wt.% (as shown in Table S1), which was slightly higher than that of the nontreated RS (30.8 wt.%). It was reported that transition metal compounds primarily existed as a metal element state at the temperature range of 600 °C to 800 °C as they were added into the biomass for catalytic pyrolysis (Glatzel *et al.* 2013; Thompson *et al.* 2015). Accordingly, the concentration of the transition metal compounds in the residue of the transition metal-treated RS can be approximately calculated, as well as the difference in the residue that originated from the RS (Δ*Residue*), which was showed in Table S1. It can be found that a positive Δ*Residue* was obtained from all transition metal-treated samples, which suggested that the char formation was actually

enhanced. This is likely due to the inhibition of the depolymerization reactions after the transition metal treatment (Collard *et al.* 2015). Similar results were found in previous studies (Collard *et al.* 2012, 2015).

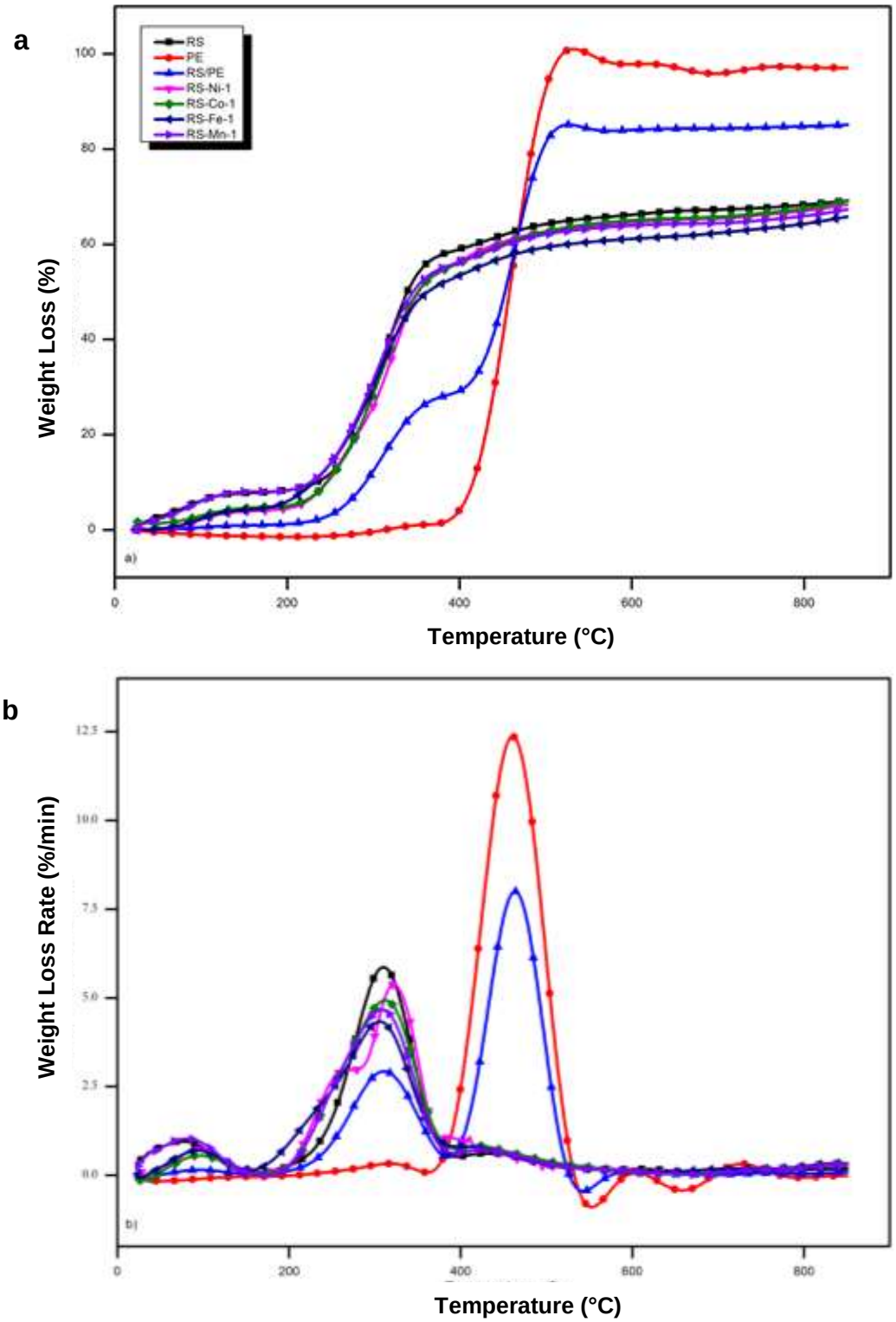

Fig. 1 Pyrolytic behavior of the RS mixtures with or without transition metal catalysts, PE, and RS/PE: a) TG curves, b) DTG curves

As shown in Fig. 1a, the PE possessed a high level of thermal stability before 350 °C with a weight loss below 1.0 wt%, which can be attributed to its highly crystalline structure. After that, it underwent a rapid weight loss stage, taking place within a narrow temperature range (400 °C to 510 °C) with 98.46 wt% weight loss. Zhang *et al.* (2016) stated that the chemical structure of PE was relatively simple compared to the biomass. As long as an adequate number of free radicals were formed, under certain condition (*i.e.*, at a relatively high temperature), the intermolecular scission and depolymerization reactions, as well as the intramolecular cleavage of PE, would easily occur (Xiong *et al.* 2015). However, the PE was completely decomposed without solid residue during this decomposition period, which was consistent with its low fixed carbon content (as shown in Table 1). The DTG curve shown in Fig. 1b further revealed that the PE showed a maximum weight loss rate of -12.36 wt%/min at 460 °C.

When the RS was pyrolyzed together with the PE (RS/PE), the corresponding pyrolysis process primarily displayed two successive weight loss stages in terms of the TG curve, as shown in Fig. 1a. The first stage started at 214 °C and ended at 367 °C and was attributed to the decomposition of the RS, while the PE decomposition process in the RS/PE mixture primarily occurred at 380 °C to 513 °C. The initial decomposition temperature of the RS in the RS/PE mixture was slightly delayed compared to the RS mixture, which may have resulted from the presence of PE. The PE gradually melted after 100 °C, which was an endothermic process as confirmed *via* DSC analysis (Kai *et al.* 2017). The formation of char after the decomposition of the RS was responsible for the decrease in the initial decomposition temperature of the PE in the mixture. According to a previous study, the pyrolysis residue of the biomass was found to promote catalyzation of the decomposition of polypropylene (Jakab *et al.* 2000). Moreover, the weight loss of RS/PE in the first decomposition stage was 25.0 wt%, which was close to the theoretical weight loss (24.9 wt%) while the loss in the second stage (56.4 wt%) was higher than the corresponding theoretical value (49.2 wt.%). Therefore, it was revealed that the PE had a slight influence on the decomposition of RS, except for the melting process. In addition, the decomposition of PE led to the further decomposition of the RS residue. This can be confirmed by the residue yield at the end of pyrolysis (14.89 wt%), which was lower than that of the theoretical one (15.4 wt%). According to the DTG curve shown in Fig. 1b, it can be seen that the decomposition of RS and PE in the mixture showed peak decomposition temperatures at 309 °C with a maximum decomposition rate of -2.93 wt%/min, and at 461 °C with a maximum decomposition rate of -8.00 wt%/min, respectively. These values are similar to those from isolated RS and PE, which revealed that the blending treatment had a slight influence on the temperature of the maximum decomposition rate of the individual components in the mixture.

RS/PE mixture with a transition metal catalyst

The TG and the DTG curves of the RS/PE mixture with or without transition metals (RS/PE, RS/PE-Ni-1, RS/PE-Co-1, RS/PE-Fe-1, and RS/PE-Mn-1) are illustrated in Fig. 2. After the transition metals treatment, the pyrolysis behavior of the RS/PE mixture presented a similar trend to the non-transition metal treated mixture (RS/PE) in terms of the TG results, which are mainly comprised of three weight loss stages. Particularly, the first stage ranging from room temperature (°C) to 163 °C was assigned to the loss of free water, while the second (152 °C to 367 °C) and third (360 °C to 513 °C) stages were attributed to the decomposition of RS and PE, respectively. It was found that the initial decomposition temperature of RS and PE in the RS/PE-Ni-1, RS/PE-Co-1,

RS/PE-Fe-1, and RS/PE-Mn-1 mixtures were reduced by varying degrees when compared with the RS/PE mixture. For example, the RS and the PE in the RS/PE-Ni-1 mixture started to decompose at 190 °C and 361 °C, respectively, which represented decreases by 24 °C and 19 °C compared to the RS/PE mixture, respectively. This result suggested that the involvement of transition metals was effective in the activation of the RS and the PE constitutes in the RS/PE mixture and promoted their decomposition. As shown in Table S1, the Δ *Residue* in the char obtained from RS/PE-Ni-1, RS/PE-Co-1, RS/PE-Fe-1, and RS/PE-Mn-1 was lower than the theoretical Δ*Residue* (negative values). A possible explanation is that the presence of the transition metals promoted the interaction between the RS and the PE to produce more volatiles regarding condensable and non-condensible products and consequently reduced the residue yield. The influence of the transition metals on the interaction between the RS and the PE followed the order: Ni > Fe > Mn > Co, in terms of Δ*Residue*.

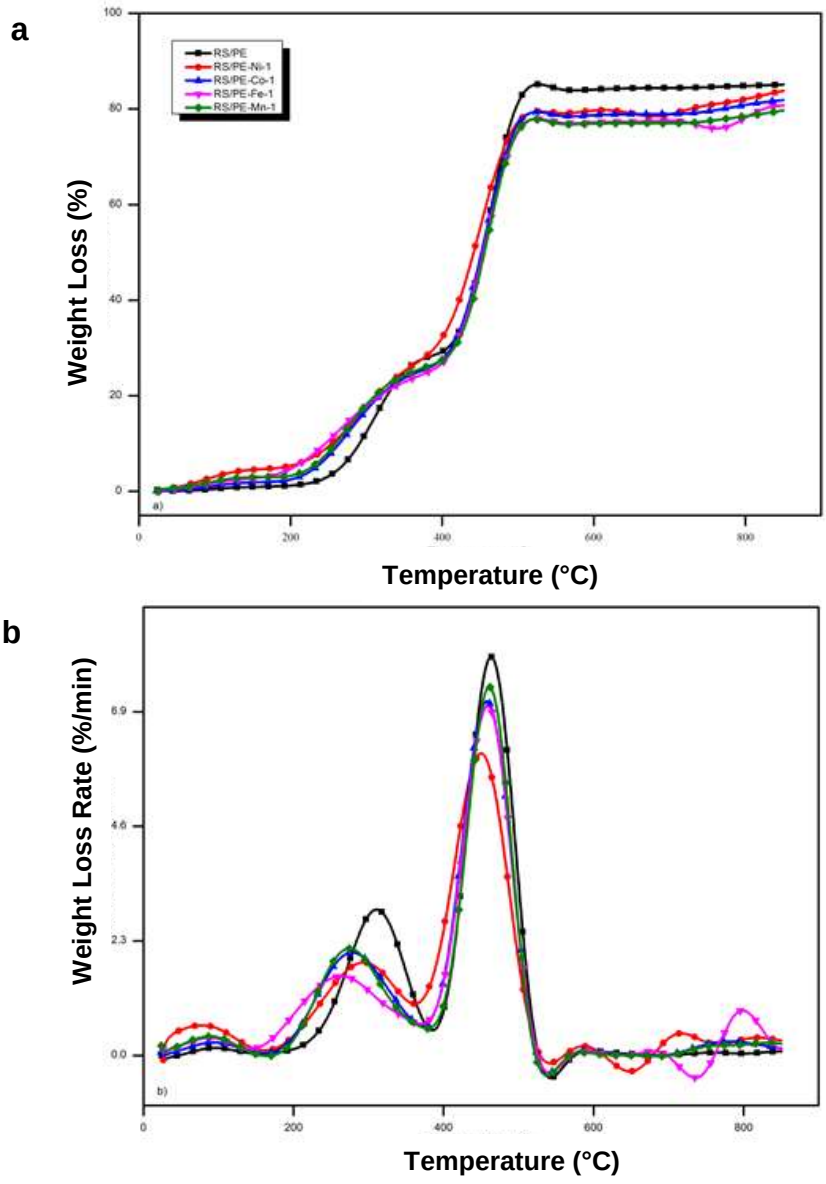

Fig. 2. Pyrolytic behavior of the RS/PE mixture with or without a transition metal catalyst: a) TG curves, b) DTG curves

The corresponding DTG curves for the RS/PE mixtures with or without a transition metal are shown in Fig. 2b. The temperature at the maximum weight loss rate for RS decreased from 309 °C for the RS/PE mixture to 293 °C, 278 °C, 259 °C, and 274 °C for the RS/PE-Ni-1, RS/PE-Co-1, RS/PE-Fe-1, and RS/PE-Mn-1 mixtures, respectively. The maximum weight loss rate for the PE in the RS/PE-Ni-1, RS/PE-Co-1, RS/PE-Fe-1, and RS/PE-Mn-1 mixtures occurred at 449 °C, 456 °C, 457 °C, and 458 °C, respectively, which was 5 °C to 14 °C lower than the RS/PE mixture. These observations suggested that the introduction of a transition metal was in favor of the decomposition of the RS and the PE in the mixture and made the decomposition peak temperature shift into a lower zone. Furthermore, it was evident that the reduction of the RS decomposition temperature (16 °C to 50 °C) in the mixture was larger than the reduction of the PE (5 °C to 14 °C) with the addition of transition metals, which indicated the response between the RS and the transition metal was relatively stronger. It was proposed that for the decomposition of RS in a transition metal-treated RS/PE mixture, the decrease in the decomposition temperature of the RS compared to a non-transition metal treated mixture was primarily due to the presence of transition metals. However, the decomposition of the PE in a transition metal-treated RS/PE mixture was affected by both the transition metals and the active oxygenated compounds (O-containing free radicals), which originated from the decomposition of the RS (Zhang *et al.* 2016; Wang *et al.* 2018). Therefore, it seems that the interaction between the RS and the transition metals was stronger than the interactions between PE, transition metals, and active oxygenated compounds.

RS/PE mixture with different levels of Ni catalyst

Figure 3 shows the TG and the DTG curves of the RS/PE mixture with different levels of Ni during pyrolysis. The weight loss of the RS/PE mixture with different levels of Ni catalyst was mainly composed of three stages, *i.e.*, room temperature (°C) to 214 °C, 190 °C to 367 °C, 360 °C to 513 °C, which were assigned to the loss of free water, the decomposition of RS, and the decomposition of PE, respectively. It was evident that the free water content in the mixtures showed a positive relationship with the level of Ni catalyst. This was due to fact that the Ni catalyst enhanced the hydrophilicity of the feedstock (especially the RS) *via* the destruction of their structures and serving as hydrophilic sites themselves (Collard *et al.* 2015). After the water loss stage, the RS in the different levels of Ni-treated RS/PE samples began to decompose. The initial decomposition temperatures were 214 °C, 202 °C, 197 °C, 194 °C, and 190 °C for RS/PE-Ni-0, RS/PE-Ni-0.25, RS/PE-Ni-0.5, RS/PE-Ni-0.75, and RS/PE-Ni-1, respectively. It appeared that when a greater amount of Ni catalyst was involved, the initial decomposition temperature was decreased. However, the decomposition of the PE during the third stage started at 380 °C for RS/PE-Ni-0, 384 °C for RS/PE-Ni-0.25, 381 °C for RS/PE-Ni-0.5, 365 °C for RS/PE-Ni-0.75, and 360 °C for RS/PE-Ni-1. This result revealed that a lower Ni catalyst content (below 0.5 mmol/g) slightly restricted the decomposition of the PE fraction in the mixtures, while decomposition was greatly promoted when the Ni catalyst content was in a range of 0.75 mmol/g to 1 mmol/g. The fact that the catalyst levels played a key role in determining the initial decomposition temperature of the individual components in the mixtures was also confirmed in a previous study (Wang *et al.* 2018). Furthermore, in terms of the residue (Table S1), the Δ*Residue* of RS/PE-Ni-0.25 was 1.14 wt.%; which indicated that the involvement of a Ni catalyst promoted the formation of char content and had a slight influence on the

interaction between the RS and the PE to produce a greater number of volatiles, as aforementioned. Afterwards, the Δ*Residue* showed negative values and gradually decreased with an increase in the Ni catalyst content in the RS/PE mixtures. This result suggests that an increase in the Ni catalyst level played a positive role in promoting interactions between the RS and the PE in the mixtures to produce a greater number of volatiles.

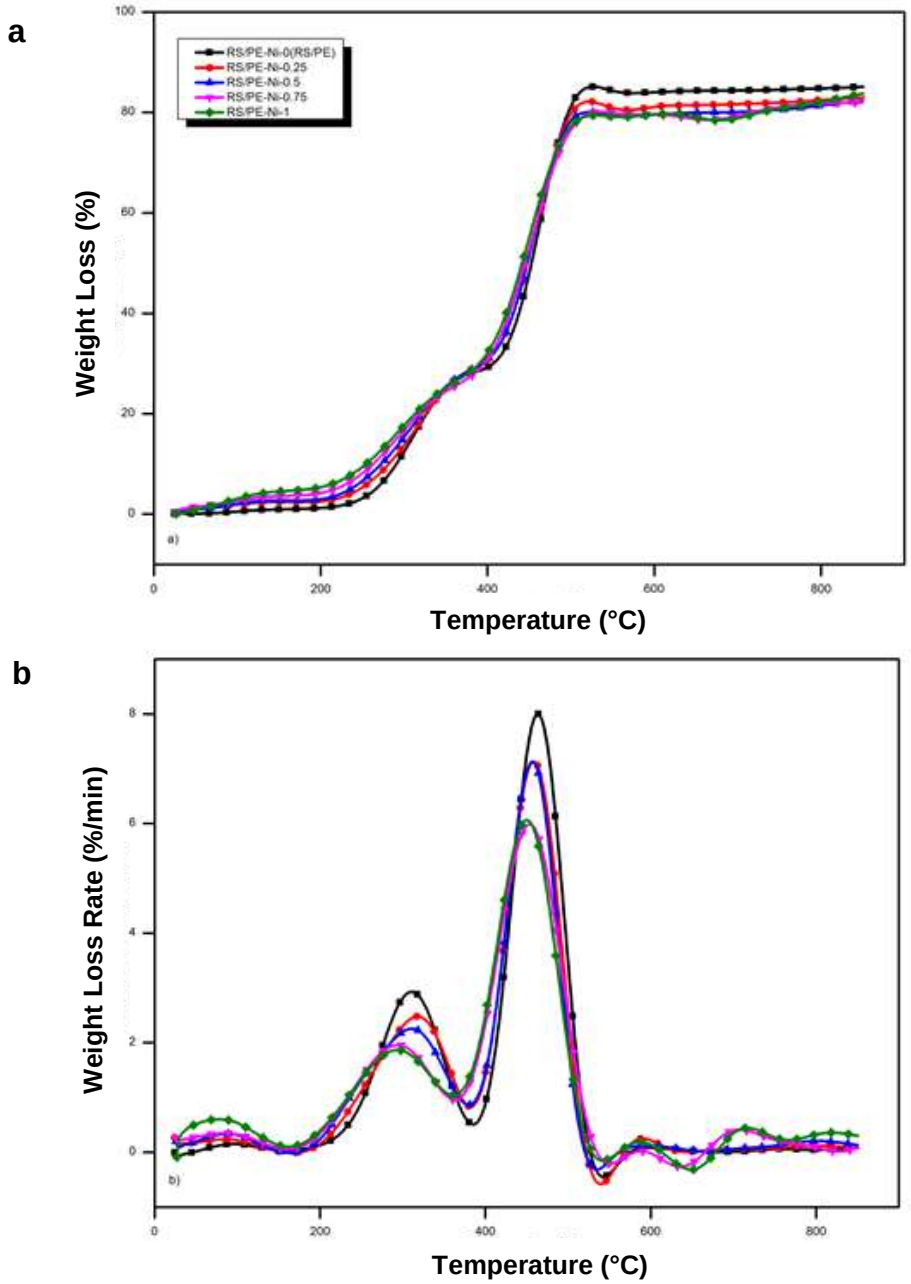

Fig. 3. Pyrolytic behavior of RS/PE mixture with different content of Ni catalyst: a) TG curves, b) DTG curves

According to the DTG results shown in Fig. 3b, the temperature of the maximum weight loss rate of RS in the RS/PE-Ni-0, RS/PE-Ni-0.25, RS/PE-Ni-0.5, RS/PE-Ni-0.75, and RS/PE-Ni-1 mixtures was 309 °C, 318 °C, 311 °C, 294 °C, and 293 °C, respectively.

The peak decomposition temperature shifted to a higher temperature when a lower Ni catalyst level was involved (less than 0.5 mmol/g), while a higher Ni catalyst level (0.75 mmol/g to 1 mmol/g) seemed to promote the decomposition of the RS at a lower temperature. In addition, the temperature of the maximum weight loss for the PE in different levels of Ni-treated mixtures showed a negative relationship with the level of Ni, which decreased from 463 °C for RS/PE-Ni-0 to 457 °C, 456 °C, 453 °C, and 449 °C for RS/PE-Ni-0.25, RS/PE-Ni-0.5, RS/PE-Ni-0.75, and RS/PE-Ni-1, respectively. Therefore, it could be concluded that when the Ni catalyst content in the RS/PE mixture was higher than 0.75 mmol/g, the catalyst would play an active role in the decomposition of the individual fractions (RS and PE), as well as the interaction between the RS and the PE.

Evaluation of the Interactions during the Co-pyrolysis of the RS and the PE

Figure 4 illustrated the variation in the ΔW in terms of temperature for the pyrolysis of the RS/PE mixtures with or without transition metals. For the RS/PE mixture, the variation in ΔW was presented as a negative value with the increase in the pyrolysis temperature from room temperature. Nevertheless, the values were below -2.0 wt% before 100 °C, which suggested that there is no distinct interaction between the RS and the PE within this temperature range (Wang *et al.* 2018). However, ΔW was still lower than -2.0 wt% when the PE in the RS/PE mixture started to soften at 100 °C (as shown in Fig. 1). When the temperature was increased to 430 °C, the ΔW of the RS/PE mixture reached a peak value of -4.01 wt%. However, with a continued increase in temperature, ΔW sharply rose and changed into a positive value after reaching 471 °C. The marked increase in the value of ΔW may be attributed to the rapid decomposition of the PE and the synergistic interaction between the PE and RS intermediates. This deduction was confirmed by Suriapparao *et al.* (2018) who revealed that the bio-oil, char, and gas yields derived from the co-pyrolysis of biomass and synthetic plastic were non-additive with respect to that obtained from individual fractions. The maximum ΔW value of the RS/PE mixture at this stage (2.86 wt%) was observed at 499 °C. Thereafter, the ΔW value slightly decreased, but it stagnated around 2.15 wt%, which could be a result of the synergistic interaction between the RS and PE residues. Accordingly, it was concluded that the synergistic interaction between the RS and the PE in the RS/PE mixture occurred almost the entire pyrolysis process.

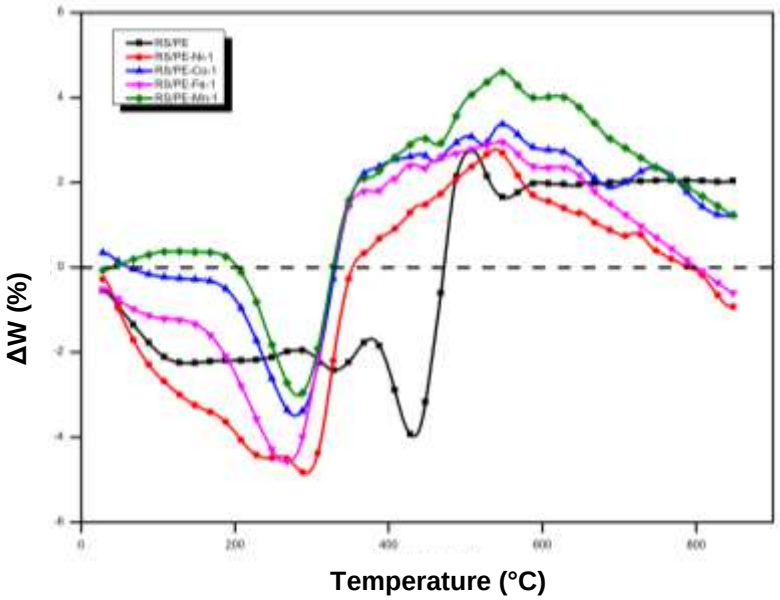

Fig. 4. Variation of the ΔW in the samples as a function of temperature

After the introduction of transition metals, the variation in Δ*W* of the RS/PE mixtures was greatly changed compared to the non-transition metal treated mixtures, which slightly varied with the type of transition metal. The Δ*W* of RS/PE-Ni-1 showed a steady decreasing trend when heated, and the minimum value of -4.91 wt% was obtained at 295 °C. In addition, the Δ*W* of RS/PE-Co-1, RS/PE-Fe-1, and RS/PE-Mn-1 had a slight fluctuation before reaching 188 °C (-0.49 wt%), 148 °C (-1.31 wt%), and 215 °C (± 0.37 wt.%), respectively. Afterwards, the Δ*W* of RS/PE-Co-1, RS/PE-Fe-1, and RS/PE-Mn-1 greatly decreased with an increase of temperature, and exhibited their minimum values of -3.50 wt% at 277 °C, -4.61 wt% at 265 °C, and -3.04 wt% at 281 °C, respectively. After the temperature corresponding to the minimum value of Δ*W*, the Δ*W* of the transition metal treated RS/PE mixtures was drastically increased. It was worth noting that the temperatures of the peak value of the Δ*W* for the transition metal treated RS/PE mixtures at this period were much lower than the non-transition metal treated mixtures, which was mainly attributed to the introduction of the transition metals. The transition metals were able to promote notable RS decomposition at relatively low temperatures, which produced more intermediates, especially oxygenated compounds, which were active in attacking the PE chain structure. However, the presence of the transition metals could intensify the synergistic interaction between the RS and PE intermediates. As a result, the softened PE coated on the surface of the RS could be readily broken though with the assistance of the transition metals, compared to the non-transition metal treated mixtures. With the gradual increase in temperature, the Δ*W* of the transition metal treated RS/PE mixtures reached maximum positive values at 535 °C, 539 °C, 541 °C, and 540 °C for RS/PE-Ni-1, RS/PE-Co-1, RS/PE-Fe-1, and RS/PE-Mn-1, respectively. These temperatures were much higher than the peak decomposition temperatures for the PE in the individual corresponding transition metal treated RS/PE mixtures (Fig. 2), which could be attributed to the strong interaction between the PE intermediates and the RS residue. In conclusion, the transition metals weakened the influence of the softened PE on the RS in the mixtures and could intensify the synergistic interaction between the RS and PE, especially after the decomposition of the PE.

Kinetic Analysis

A first-order model was conducted to fit the main decomposition stage of RS with or without transition metals, PE, and RS/PE mixture. The fit results of $\ln[-\ln(1-x)/T^2]$ versus $1/T$ and the corresponding kinetic parameters (E and A) are presented in Fig. 5 and Table 2, respectively. It can be seen that all data can be well described by the first-order model in terms of the coefficient of determination (R^2), which was in the range 0.9819 to 0.9971. In particular, RS, PE, RS-Ni-1, RS-Co-1, RS-Fe-1, and RS-Mn-1 could be fit by a single first-order reaction, while two successive first–order reactions were needed for the description of the RS/PE mixture. Similar results were observed in previous studies (Zhang *et al.* 2016; Wang *et al.* 2018). As shown in Table 2, the E value of RS was 42.3 kJ/mol. After the introduction of transition metals, the E value of the RS mixture slightly decreased. This result confirmed that the presence of transition metals was in favor of the decomposition of RS. According to the E value, the efficiency of the transition metals employed on the decomposition of RS were as follows; Fe was greater than Mn, which was greater than Ni, which was greater than Co. However, PE possessed a high E value of 165.4 kJ/mol. For the RS/PE mixture, the E of the RS increased to 32.0%, and the PE greatly decreased approximately two-fold, when compared to the isolated samples. This observation was in accordance with the results shown in Figs. 1 and 4, which suggested that the presence of PE inhibited the decomposition of RS, while the decomposition products of RS was favorable for the degradation of PE.

Table 2. Kinetic Parameters for the Pyrolysis of Samples Including RS with or Without a Catalyst, PE, and RS/PE

Material	Temperature	Conversion Range (x, %)	E (kJ/mol)	A (min^{-1})	R^2
RS	190 to 513	80.77	42.31	1.81×10^3	0.9908
RS-Ni-1	194 to 489	84.84	40.59	6.03×10^2	0.9974
RS-Co-1	197 to 520	84.52	41.81	8.25×10^2	0.9947
RS-Fe-1	176 to 490	82.68	36.70	1.82×10^2	0.9971
RS-Mn-1	199 to 509	80.38	39.56	2.31×10^2	0.9918
PE	388 to 520	98.95	165.37	1.48×10^{11}	0.9913
RS/PE	218 to 385	31.56	55.84	3.70×10^3	0.9948
	385 to 513	65.93	98.50	2.67×10^6	0.9819
Note: RS-metal-X represents the metal content in 1 g RS is X mmol.					

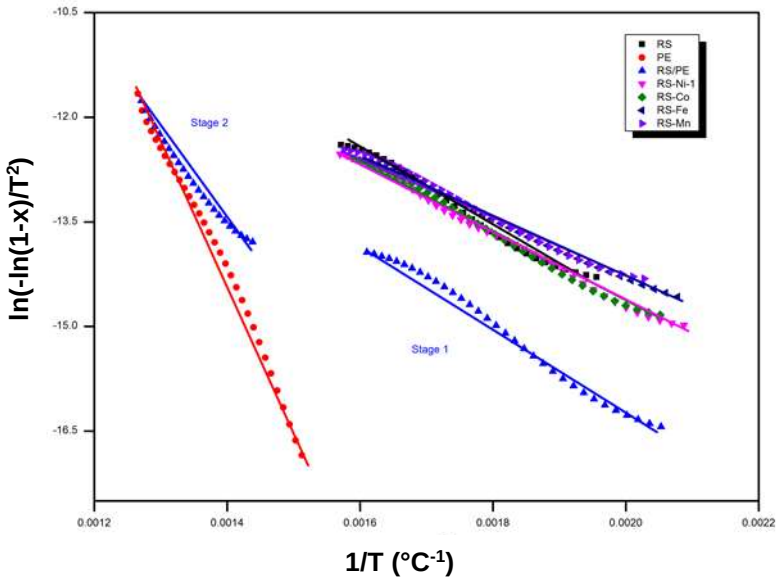

Fig. 5. Plots of ln(-ln(1-*x*)/T^2) vs 1/*T* of RS with or without a catalyst, PE, and RS/PE

Compared to RS/PE, the *E* value for the RS in the transition metal treated RS/PE mixture greatly decreased as follows; RS/PE was greater than RS/PE-Co-1, which was approximately equal to RS/PE-Mn-1, which was greater than RS/PE-Fe-1, which was approximately equal to RS/PE-Ni-1. Particularly, the influence of Ni and Fe on the decrease in the *E* value of the RS in RS/PE was superior to Co and Mn, and the *E* value of the RS in RS/PE-Ni-1 and RS/PE-Fe-1 was found to decrease by approximately two-and-a-half-fold. However, the transition metal treatment also had an influence on the reduction of the *E* value of the PE in the RS/PE mixture. The RS/PE-Ni-1 mixture showed the lowest *E* value for PE compared to the RS/PE mixture, followed by the RS/PE-Co-1, the RS/PE-Fe-1, and the RS/PE-Mn-1 mixtures. In combination the results for the influence of the introduction of transition metals on the *E* value of the RS in the RS/PE mixture, it can be concluded that Ni was found to be the best of the transition metals introduced, and possessed the strongest catalytic capability in decreasing the *E* value of RS and PE.

Table 3. Kinetic Parameters for the Pyrolysis of Samples including the RS/PE Mixtures with Different types of Catalyst

Material	Temperature	Conversion Range (x,%)	E (kJ/mol))
RS/PE	218 to 385	31.56	55.84
	385 to 513	65.93	98.50
RS/PE-Ni-1	190 to 361	25.40	20.88
	361 to 510	62.46	62.91
RS/PE-Co-1	190 to 371	28.03	37.06
	371 to 512	65.55	81.91
RS/PE-Fe-1	152 to 370	26.52	22.68
	370 to 508	65.18	82.72
RS/PE-Mn-1	198 to 377	28.54	35.36
	377 to 508	64.05	91.31
Note: RS/PE-metal-X represents the metal content in 1 g RS/PE is X mmol.			

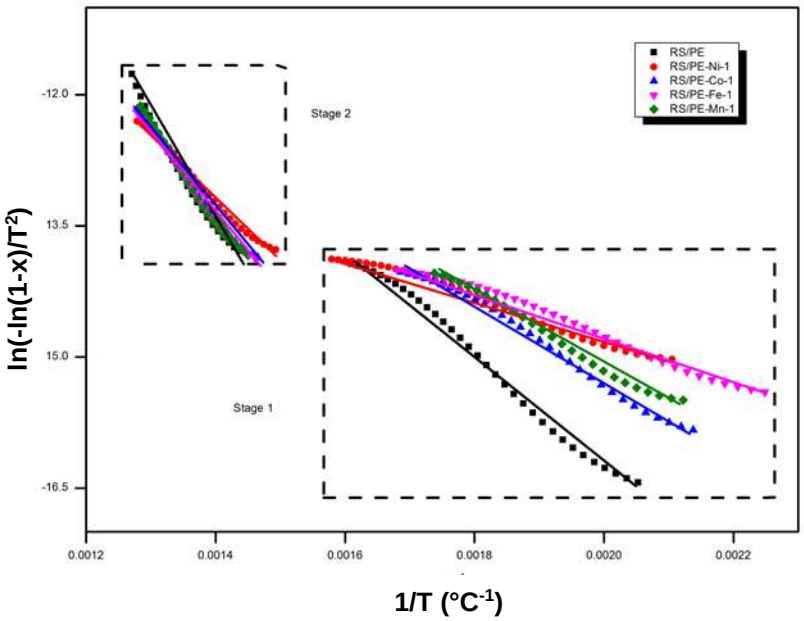

Fig. 6. Plots of ln (-ln(1-*x*)/T^2) vs 1/*T* of the RS/PE mixture with or without a transition metal catalyst

In terms of the influence of the level of transition metal in the sample, the *E* value of both the RS and the PE showed a distinct negative relationship with the level of Ni involved. In a previous study, the authors found that the addition of a greater amount of catalyst in a mixture of cellulose and PE was in favor of the decomposition of cellulose, but not the decomposition of the PE in the mixture (Wang *et al.* 2018). Zhou *et al.* (2017) revealed that an increase in the potassium levels of the wood sawdust/low density polyethylene mixtures led to an increasing trend for the *E* value of the wood sawdust but resulted in a decreasing tread in the *E* value of the low-density polyethylene. When the Ni content was 1 mmol/g (RS/PE-Ni-1), the RS and the PE in the RS/PE mixture possessed the lowest *E* value. Furthermore, the linear fit for the *E* value of the RS and the PE in different Ni content-treated RS/PE mixtures *versus* the corresponding Ni content was 0.9062 and 0.9674, respectively, which indicated that there was a direct relationship between the *E* value and the level of Ni content employed.

Table 4. Kinetic Parameters for the Pyrolysis of Samples including the RS/PE Mixtures with Different Catalyst Amounts

Material	Temperature	Conversion Range (x, %)	*E* (kJ/mol)	*A* (min^{-1})	R^2
RS/PE-Ni-0 (RS/PE)	218 to 385	31.56	55.84	3.70×10^3	0.9948
	385 to 513	65.93	98.50	2.67×10^6	0.9819
RS/PE-Ni-0.25	202 to 381	31.71	37.08	5.70×10^1	0.9963
	226 to 336	63.06	83.86	2.33×10^5	0.9806
RS/PE-Ni-0.5	419 to 496	31.25	32.88	2.38×10^1	0.9962
	197 to 380	61.65	80.90	1.38×10^5	0.9865
RS/PE-Ni-0.75	194 to 363	26.47	27.04	6.4×10^0	0.9915
	363 to 520	65.79	69.59	1.85×10^4	0.9941
RS/PE-Ni-1	190 to 361	25.40	20.88	1.37×10^0	0.9884
	361 to 510	62.46	62.91	5.66×10^3	0.9912
Note: RS/PE-metal-X represents the metal content in 1 g RS/PE is X mmol.					

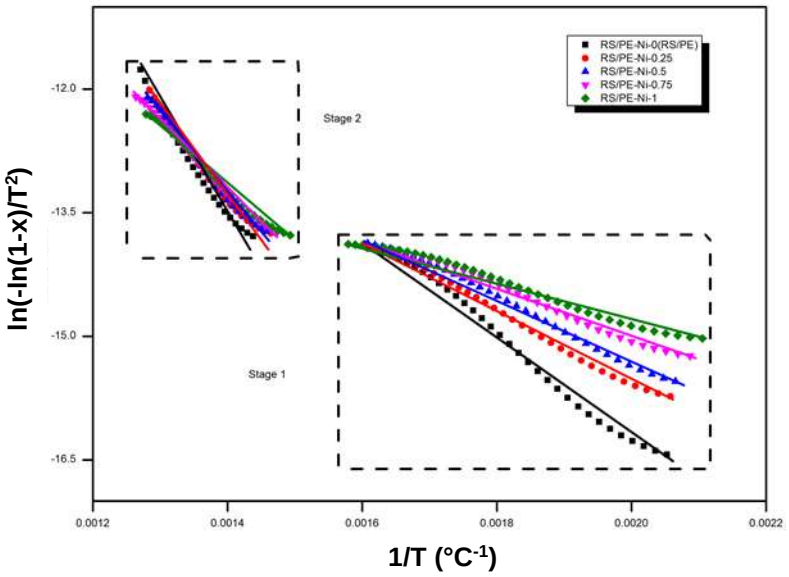

Fig. 7. Plots of ln(-ln(1-*x*)/T^2) vs 1/*T* of the RS/PE mixture with different levels of the Ni catalyst

CONCLUSIONS

1. The initial decomposition temperature of the rice straw (RS) and the polyethylene (PE) in the RS/PE-Ni-1, RS/PE-Co-1, RS/PE-Fe-1, and RS/PE-Mn-1 mixtures was reduced by varying degrees in comparison to the RS/PE mixture. In addition, the introduction of transition metals led to a reduction in the residue yield, from 14.9 wt% for the RS/PE mixture to 12.6 wt% to 14.5 wt%. In terms of the transition metal content, a lower Ni catalyst level (less than 0.5 mmol/g) slightly restricted the decomposition of the PE fraction in the mixture, while decomposition was greatly promoted when the Ni catalyst level was in the range of 0.75 mmol/g to 1 mmol/g.
2. The ΔW suggested that the introduction of transition metals could greatly weaken the influence of the softened PE on the RS in the mixture and intensify the synergistic interaction between the RS and the PE, especially after the decomposition of PE.
3. The kinetic analysis revealed that the pyrolysis of RS, PE, and transition metal treated RS could be well fit by a single first order reaction, while two consecutive first order reactions were needed to exactly describe the co-pyrolysis of the RS/PE mixture with or without transition metals. The RS/PE-Ni-1 mixture possessed the lowest E value for RS and PE, when compared to the RS/PE mixture and other transition metal-treated RS/PE mixtures. Moreover, the Ni content showed a prominent negative relationship with the E value of both the RS and the PE in the mixture.

ACKNOWLEDGMENTS

The authors greatly acknowledge the funding support from the projects supported by the National Natural Science Foundation of China (Grant no. 51676047 and 5181101221), the Scientific Research Foundation of the Graduate School of Southeast

University (YBJJ1808), and the Royal Society International Exchange Scheme (IE150760). Financial support from the China Scholarship Council are also deeply acknowledged by the authors.

REFERENCES CITED

ASTM D1762-84 (2013). "Standard test method for chemical analysis of wood charcoal," ASTM International, West Conshohocken, PA.

Collard, F., Bensakhria, A., Drobek, M., Volle, G., and Blin, J. (2015). "Influence of impregnated iron and nickel on the pyrolysis of cellulose," *Biomass and Bioenergy* 80, 52-62. DOI: 10.1016/j.biombioe.2015.04.032

Collard, F., Blin, J., Bensakhria, A., and Valette, J. (2012). "Influence of impregnated metal on the pyrolysis conversion of biomass constituents," *Journal of Analytical and Applied Pyrolysis* 95, 213-226. DOI: 10.1016/j.jaap.2012.02.009

Castro, R. C. A., Fonseca, B. G., dos Santos, H. T. L., Ferreira, I. S., Mussatto, S. I., and Roberto, I. C. (2017). "Alkaline deacetylation as a strategy to improve sugars recovery and ethanol production from rice straw hemicellulose and cellulose," *Industrial Crops and Products* 106, 65-73. DOI: 10.1016/j.indcrop.2016.08.053

Dorado, C., Mullen, C. A., and Boateng, A. A. (2015). "Origin of carbon in aromatic and olefin products derived from HZSM-5 catalyzed co-pyrolysis of cellulose and plastics *via* isotopic labeling," *Applied Catalysis B: Environmental* 162, 338-345. DOI: 10.1016/j.apcatb.2014.07.006

EPA 6010D (SW-846) (2014). "Inductively coupled plasma – atomic emission spectrometry," EPA, Washington, DC, USA.

Fermoso, J., Hernando, H., Jana, P., Mereno, I., Přech, J., Ochoa-Hernández, C., Pizarro, P., Coronado, J. M, Čejka, J., and Serrano, D. P. (2016). "Lamellar and pillared ZSM-5 zeolites modified with MgO and ZnO for catalytic fast-pyrolysis of eucalyptus woodchips," *Catalysis Today* 277(part 1) 171-181. DOI: 10.1016/j.cattod.2015.12.009

Garba, M. U., Inalegwu, A., Musa, U., Aboje, A. A., Kovo, A. S., and Adeniyi, D. O. (2018). "Thermogravimetric characteristic and kinetic of catalytic co-pyrolysis of biomass with low- and high-density polyethylenes," *Biomass Conversion and Biorefinery* 8(1), 143-150. DOI: 10.1007/s13399-017-0261-y

Glatzel, S., Schnepp, Z., and Giordano, C. (2013). "From paper to structured carbon electrodes by inkjet printing," *Angewandte Chemie International Edition* 52(8), 2355-2358. DOI: 10.1002/anie.201207693

Hernando, H., Jiménez-Sánchez, S., Fermoso, J., Pizarro, P., Coronado, J. M., and Serrano, D. P. (2016). "Assessing biomass catalytic pyrolysis in terms of deoxygenation pathways and energy yields for the efficient production of advanced biofuels," *Catalysis Science & Technology* 6(8), 2829-2843. DOI: 10.1039/C6CY00522E

Jakab, E., Várhegyi, G., and Faix, O. (2000). "Thermal decomposition of polypropylene in the presence of wood-derived materials," *Journal of Analytical and Applied Pyrolysis* 56(2), 273-285. DOI: 10.1016/S0165-2370(00)00101-7

Kai, X., Li, R., Yang, T., Shen, S., Ji, Q., and Zhang, T. (2017). "Study on the co-pyrolysis of rice straw and high density polyethylene blends using TG-FTIR-MS,"

Energy Conversion and Management 146, 20-33. DOI: 10.1016/j.enconman.2017.05.026

Kim, Y., Lee, H. W., Choi, S. J., Jeon, J., Park, S. H., Jung, S., Kim, S. C., and Park, Y. (2017). "Catalytic co-pyrolysis of polypropylene and *Laminaria japonica* over zeolitic materials," *International Journal of Hydrogen Energy* 42(29), 18434-18441. DOI: 10.1016/j.ijhydene.2017.04.139

Lee, H. W., Kim, Y., Jae, J., Jeon, J., Jung, S., Kim, S. C., and Park, Y. (2016). "Production of aromatic hydrocarbons via catalytic co-pyrolysis of torrefied cellulose and polypropylene," *Energy Conversion and Management* 129, 81-88. DOI: 10.1016/j.enconman.2016.10.001

Li, X., Li, J., Zhou, G., Feng, Y., Wang, Y., Yu, G., Deng, S., Huang, J., and Wang, B. (2014). "Enhancing the production of renewable petrochemicals by co-feeding of biomass with plastics in catalytic fast pyrolysis with ZSM-5 zeolites," *Applied Catalysis A: General* 481, 173-182. DOI: 10.1016/j.apcata.2014.05.015

Qiu, H., Sun, L., Xu, X., Cai, Y., and Bai, J. (2014). "Potentials of crop residues for commercial energy production in China: A geographic and economic analysis," *Biomass and Bioenergy* 64, 110-123. DOI: 10.1016/j.biombioe.2014.03.055

Sipra, A. T., N. Gao, and H., Sarwar (2018). "Municipal solid waste (MSW) pyrolysis for bio-fuel production: a review of effects of MSW components and catalysts," *Fuel Processing Technology* 175, 131-147. DOI: 10.1016/j.fuproc.2018.02.012

Suriapparao, D. V., Boruah, B., Raja, D., and Vinu, R. (2018). "Microwave assisted co-pyrolysis of biomasses with polypropylene and polystyrene for high quality bio-oil production," *Fuel Processing Technology* 175, 64-75. DOI: 10.1016/j.fuproc.2018.02.019

Thompson, E., Danks, A. E., Bourgeois, L., and Schnepp, Z. (2015). "Iron-catalyzed graphitization of biomass," *Green Chemistry* 17(1), 551-556. DOI: 10.1039/C4GC01673D

Uzun, B. B., and Yaman, E. (2017). "Pyrolysis kinetics of walnut shell and waste polyolefins using thermogravimetric analysis," *Journal of the Energy Institute* 90(6), 825-837. DOI: 10.1016/j.joei.2016.09.001

Wang, Q., Hu, J., Shen, F., Mei, Z., Yang, G., Zhang, Y., Hu, Y., Zhang, J., and Deng, S. (2016). "Pretreating wheat straw by the concentrated phosphoric acid plus hydrogen peroxide (PHP): Investigations on pretreatment conditions and structure changes," *Bioresource Technology* 199, 245-257. DOI: 10.1016/j.biortech.2015.07.112

Wang, Z., Shen, D., Wu, C., and Gu, S. (2018). "Thermal behavior and kinetics of co-pyrolysis of cellulose and polyethylene with the addition of transition metals," *Energy Conversion and Management* 172, 32-38. DOI: 10.1016/j.enconman.2018.07.010

Xiang, Z., Liang, J., Morgan Jr., H. M., Liu, Y., Mao, H., and Bu, Q. (2018). "Thermal behavior and kinetic study for co-pyrolysis of lignocellulosic biomass with polyethylene over cobalt modified ZSM-5 catalyst by thermogravimetric analysis," *Bioresource Technology* 247, 804-811. DOI: 10.1016/j.biortech.2017.09.178

Xiong, S., Zhuo, J., Zhou, H., Pang, R., and Yao, Q. (2015). "Study on the co-pyrolysis of high density polyethylene and potato blends using thermogravimetric analyzer and tubular furnace," *Journal of Analytical and Applied Pyrolysis* 112, 66-73. DOI: 10.1016/j.jaap.2015.02.020

Yang, H., Yan, R., Chen, H., Zheng, C., Lee, D. H., Liang, D. T. (2006). "Influence of mineral matter on pyrolysis of palm oil wastes," *Combustion and Flame* 146(4), 605-611. DOI: 10.1016/j.combustflame.2006.07.006

Zhang, L., Liu, R., Yin, R., and Mei, Y. (2013). "Upgrading of bio-oil from biomass fast pyrolysis in China: A review," *Renewable and Sustainable Energy Reviews* 24, 66-72. DOI: 10.1016/j.biortech.2017.09.178

Zhang, Q., Huang, H., Han, H., Qiu, Z., and Achal, V. (2017). "Stimulatory effect of in-situ detoxification on bioethanol production by rice straw," *Energy* 135, 32-39. DOI: 10.1016/j.energy.2017.06.099

Zhang, X., Lei, H., Chen, S., and Wu, J. (2016). "Catalytic co-pyrolysis of lignocellulosic biomass with polymers: A critical review," *Green Chemistry* 18(15), 4145-4169. DOI: 10.1039/C6GC00911E

Zhang, X., Lei, H., Zhu, L., Zhu, X., Qian, M., Yadavalli, G., Wu, J., and Chen, S. (2016). "Thermal behavior and kinetic study for catalytic co-pyrolysis of biomass with plastics," *Bioresource Technology* 220, 233-238. DOI: 10.1016/j.biortech.2016.08.068

Zhou, L., Zou, H., Wang, Y., Le, Z., Liu, Z., and Adesina, A. A. (2017). "Effect of potassium on thermogravimetric behavior and co-pyrolytic kinetics of wood biomass and low density polyethylene," *Renewable Energy* 102(Part A), 134-141. DOI: 10.1016/j.renene.2016.10.028

Article submitted: July 24, 2019; Peer review completed: September 8, 2019; Revised version received: September 20, 2019; Accepted: September 22, 2019; Published: September 26, 2019.
DOI: 10.15376/biores.14.4.9033-9053